Journal of Macromolecular Science, Part A
Publication details, including instructions for authors and subscription information:
http://www.informaworld.com/smpp/title~content=t713597274

Preparation of Conducting Polyaniline and Polyaniline- Fluorinated Montmorillonite Nanocomposites in Supercritical Carbon Dioxide

Fu Sun[ab]; Yuejin Pan[c]; Jing Wang[ab]; Zi Wang[ab]; Chunpu Hu[ab]; Qingzhi Dong[ab]
[a] School of Materials Science and Engineering, East China University of Science and Technology, Shanghai, People's Republic of China [b] Key Laboratory for Ultrafine Materials of Ministry of Education, Shanghai, People's Republic of China [c] Shanghai Zhongda Technology Corporation, Shanghai, People's Republic of China

To cite this Article Sun, Fu , Pan, Yuejin , Wang, Jing , Wang, Zi , Hu, Chunpu and Dong, Qingzhi(2009) 'Preparation of Conducting Polyaniline and Polyaniline- Fluorinated Montmorillonite Nanocomposites in Supercritical Carbon Dioxide', Journal of Macromolecular Science, Part A, 46: 1, 37 — 45
To link to this Article: DOI: 10.1080/10601320802515159
URL: http://dx.doi.org/10.1080/10601320802515159

Journal of Macromolecular Science®, Part A: Pure and Applied Chemistry (2009) **46**, 37–45

ISSN: 1060-1325 print / 1520-5738 online
DOI: 10.1080/10601320802515159

Taylor & Francis
Taylor & Francis Group

Preparation of Conducting Polyaniline and Polyaniline-Fluorinated Montmorillonite Nanocomposites in Supercritical Carbon Dioxide

FU SUN,[1,3] YUEJIN PAN,[2] JING WANG,[1,3] ZI WANG,[1,3] CHUNPU HU[1,3] and QINGZHI DONG[1,3,*]

[1]*School of Materials Science and Engineering, East China University of Science and Technology, Shanghai 200237, People's Republic of China*
[2]*Shanghai Zhongda Technology Corporation, Shanghai 201702, People's Republic of China*
[3]*Key Laboratory for Ultrafine Materials of Ministry of Education, Shanghai 200237, People's Republic of China*

Received May 2008, Accepted July 2008

A new polymerization procedure with the aid of reverse micelles in supercritical carbon dioxide ($SCCO_2$) has been employed to synthesize polyaniline (PANI). Sodium bis(2-ethylhexyl)-sulfosuccinate (AOT) and polyether-modified polysiloxane (PeSi) were used as mixing surfactants. PANI with more favorable needle-like aggregation structure, higher crystallinity, more excellent conductivity (7.22 S cm^{-1}) and better dispersibility in ethanol has been obtained via the inverse emulsion polymerization in $SCCO_2$, compared to the PANI synthesized in isooctane. These results were demonstrated by the analysis of Fourier Transform Infrared Spectroscopy (FTIR), Scanning Electron Microscope (SEM), Transmission Electron Microscope (TEM), X-ray diffraction patterns (XRD) and conductivity measurement. The new polymerization procedure was also employed to prepare polyaniline-fluorinated montmorillonite (PANI-FMMT) nanocomposites in $SCCO_2$. The nanocomposites with highly concentrated (12 wt%–50 wt% loading to monomer), fully delaminated FMMT were successfully prepared. The intercalation of FMMT in $SCCO_2$ was characterized by FTIR, XRD, TEM. Thermogravimetry Analysis (TGA) was performed to investigate the enhancement of thermal stability of PANI-FMMT nanocomposites. $SCCO_2$ facilitate the synthesis of PANI with high performance and PANI-MMT with high MMT concentration. $SCCO_2$ is not only an "alternative" solvent for its environmental-friendly characteristic, but also a more "effective" medium compared to some organic solvent (such as isooctane) to prepare PANI and its intercalated composite materials.

Keywords: Supercritical carbon dioxide ($SCCO_2$), polyaniline (PANI), fluorinated montmorillonite (FMMT), inverse emulsion, nanocomposites

1 Introduction

Supercritical carbon dioxide ($SCCO_2$) has emerged as important supercritical fluids (SCF) in the past decade, due to its many desirable attributes such as low cost, abundance, low toxicity, and readily accessible supercritical conditions ($T_c = 31.1°C$, $P_c = 7.38$ MPa). It has been used as environmentally friendly solvent for a range of materials synthesis and process applications (1, 2). Many investigators have demonstrated the feasibility of polymerization in $SCCO_2$, but $SCCO_2$ is always employed as "alternative" or "green" solvent, instead of "effective" medium (3–8).

In fact, $SCCO_2$ offers mass transfer property advantages over conventional organic solvents because of their high diffusivity, liquid-like density, low viscosity, near-zero surface tension and strong solvent power for many organic compounds. The utility of $SCCO_2$ as a delaminating agent for layered materials has been possible and several researchers have successfully synthesized some conducting polymer (9) and intercalated some polymers into montmorillonite (MMT) via a $SCCO_2$-mediated process (10–14).

Polyaniline (PANI) is one of the most widely studied conducting polymers because of its environmental stability, excellent electrical properties, plastic nature, economical efficiency, ease of preparation and other versatile potential performance. It has been proposed for applications such as anti-static additives, corrosion inhibition coatings, electrochromic display, sensors, light-emitting diodes, capacitors, rechargeable batteries, solar

*Address correspondence to: Qingzhi Dong, School of Materials Science and Engineering, East China University of Science and Technology, Shanghai 200237, People's Republic of China and Key Laboratory for Ultrafine Materials of Ministry of Education, Shanghai 200237, People's Republic of China. E-mail: qzhdong@ecust.edu.cn

cells, gas permeation membranes and electromagnetic interference shielding materials, etc. (15–17). In recent years, PANI/MMT composites have attracted more and more attention, the layered complex can benefit from the properties of both PANI and MMT. The combination of the organic and inorganic materials can lead to a high degree of polymer ordering, exhibit thermal stability and enhanced mechanical properties. Furthermore, it reveals novel properties due to the synergistic effect of the two components (18–22). Different polymerization methods were researched to synthesize PANI and its composites, such as solution polymerization, dispersion polymerization and emulsion polymerization. Inverse microemulsion polymerization has attracted much interest because a variety of reactants can be concentrated and introduced into the nanometer-sized aqueous domains to control the structure and property of materials (23–25).

In this paper, we report a novel procedure to prepare PANI and polyaniline-fluorinated montmorillonite (PANI-FMMT) nanocomposites with the aid of reverse micelles in $SCCO_2$ at room temperature, using inexpensive non-fluorous sodium bis(2-ethylhexyl)-sulfosuccinate (AOT) and polyether-modified polysiloxane (PeSi) as surfactants. Inverse emulsion polymerization of aniline in $SCCO_2$ is analogous to that in organic solvent, where reactants are concentrated, the quantity of acid can be reduced, monomer and other additives can be dispersed homogeneously (23–25).

2 Experimental

2.1 Materials

Aniline, ammonium peroxydisulphate (APS), ethanol, sodium bis(2-ethylhexyl)-sulfosuccinate (AOT), and hydrochloric acid (HCl) were purchased from Sinopharm Chemical Reagent Company. The Na-montmorillonites (NaMMT) (Cation Exchange Capacities CEC = 110 mmol/100g) and cetyl trimethyl ammonium bromide (CTAB) used in this study were purchased from Zhengjiang Fenghong Chemicals Company (China). Perfluoroalkyl-sulfonyl quaternary ammonium iodides (FCAI) was supplied by Heide Chemical Development Company (China). Polyether-modified polysiloxane (PeSi) was obtained from ShinEtsu Company (Japan). CO_2 with a purity of 99.95% was a commercial product. Aniline was distilled under reduced pressure and stored in a refrigerator before use. All other reagents of analytical grade were used as received.

2.2 Fluorinated Modification of MMT

Fluorinated MMT (FMMT) were prepared by a cation-exchange reaction between the sodium cations of NaMMT and FCAI. The intercalation process was described as follow: A suspension of NaMMT in distilled water (5 g/500 mL) was swelled overnight, then an ethanol solution of the FCAI with equivalent amount of the CEC of NaMMT in the suspension was added and stirred for 12 h at 80°C. Subsequently, it was collected by filtration, the powder was washed with hot deionized water and ethanol several times until there was no white precipitate observed by an $AgNO_3$ test. The solid was dried in vacuum and ground in an agate mortar for further experimentation. The organic MMT (OMMT) was prepared using an analogous procedure, but CTAB was selected as intercalation agent instead of FCAI.

2.3 Synthesis of PANI and PANI-FMMT in $SCCO_2$

In a typical experiment, 2 g AOT and 1.5 g PeSi was dissolved in 8 ml ethanol, the solution was denoted as (A). A controlled amount of distilled water (water solubilization factor $w_0 = [H_2O]/[AOT] = 74$), 1.1 g (0.0118 mol) aniline, FMMT and hydrochloric acid solution (4M, the mole ratio of HCl and ANI was 2.5) were mixed with sonication for 1 h, the mixture was denoted as (B), (A) and (B) were injected into a 125 mL view autoclave containing a magnetic stir bar. 1.08 g (0.00472 mol) APS was dissolved in 3 mL distilled water, before they were poured into a small glass container with several small holes on the bottom. The holes were coated with a little inert silicone grease. The container was placed in the autoclave. The schematic diagram of the apparatus is shown in Figure 1. The autoclave was first purged with a flow of CO_2 to remove air for 10 min and filled with liquid CO_2 by an automatic syringe pump, then it was placed in a constant temperature water bath of 35°C, the pressure in the autoclave increased to 30 ± 2MPa. The inverse emulsion of hydrochloric aniline was stabilized by AOT, PeSi and ethanol, and they were mixed with FMMT uniformly in $SCCO_2$ with continuous 600 rpm stirring. After a period of time, the silicone grease was swelled and damaged by $SCCO_2$, the aqueous solution of APS exuded from the holes of the small glass container. The micro aqueous droplets containing APS contacted the micelles of aniline and initiated the polymerization. The polymerization was allowed to proceed for 24 h, then the autoclave was cooled to room temperature and the CO_2 was slowly vented through a pressure release valve. A large amount of ethanol was added to the dark green reaction mixture, then the mixture was filtered, washed with ethanol and deionized water in order to remove unreacted monomer and surfactants, finally dried under vacuum at 50°C. The samples were denoted as PANI-FMMTX-SC, where X means the mass ratio of FMMT to aniline monomer. The pure PANI without FMMT was synthesized by the same inverse emulsion polymerization procedure and the sample was denoted as PANI-SC. All pure PANI and PANI in composites are in emeraldine salt state.

As the control experiments, the conventional inverse emulsion polymerization was carried out using an analogous procedure under nitrogen atmosphere, the OMMT

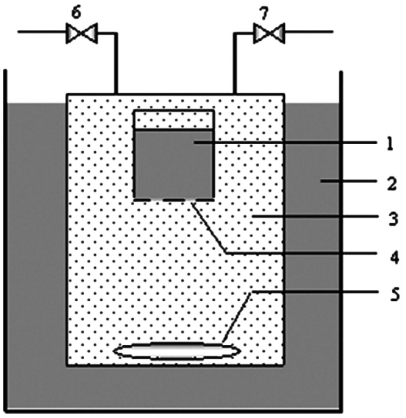

Fig. 1. Schematic diagram of the apparatus 1. aqueous solution of APS 2. water bath 3. inverse emulsion of aniline aided by AOT, PeSi and ethanol in $SCCO_2$ in a view autoclave 4. small holes coated with a little inert silicone grease 5. magnetic stir bar 6. and 7. valves.

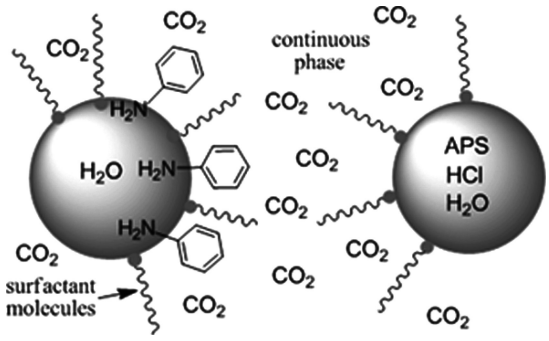

Fig. 2. Schematic diagram of the reaction location in $SCCO_2$. Depiction of two separated parts of reverse micelles containing monomer and APS, respectively, aniline hydrochloride were distributed at $SCCO_2$/water interface. No micelle shape is implied. The diagram is not to scale.

and isooctane were adopted instead of FMMT and $SCCO_2$. The samples were denoted as PANI-OMMTX-CON and PANI-CON, respectively.

2.4 Characterization Methods

Fourier transform infrared spectroscopy (FTIR, Nicolet 5700) of the samples were recorded using KBr pellets method to determine the chemical structure of PANI and the nanocomposites. X-ray powder diffraction patterns (XRD) of samples were obtained on a Rigaku diffractometer (D/MAX 2550 VB/PC) using CuKα radiation (0.154 nm, 40 kV, 100 mA, 0.5°/min). Transmission electron microscopy (TEM, JEOL JEM-2010) was used with an acceleration voltage of 120 kV to observe the morphology of the samples which were prepared by evaporation of a drop of diluted ethanol dispersions onto a 200 mesh copper grid. Scanning electron microscope (SEM, JSM-6360LV) was used to examine the morphology of samples which were mounted onto aluminum studs and sputter-coated with gold. Thermogravimetric analysis (TGA, TA model 2050) was carried out at a heating rate of 10°C/min from room temperature to 800°C under nitrogen atmosphere. DC conductivity of room temperature measurements were performed by conventional four-probe technique.

3 Results and Discussion

3.1 Location of the Polymerization

AOT is an anionic surfactant to form reverse micelles in nonpolar solvent, as well as $SCCO_2$ with many good qualities (26–28). PeSi is a nonionic surfactant with CO_2-philic silicone molecule chain and it has been confirmed to be effective for emulsion polymerization of vinyl pyrrolidone in $SCCO_2$ (29, 30). In our experiment, AOT and PeSi were selected as mixed surfactants and ethanol as co-surfactant to enhance the stability of reverse micelles in $SCCO_2$. PANI was chemically synthesized by mixing two separate parts of water-in-$SCCO_2$ reverse micelles. These two parts contained aniline hydrochloride and oxidant APS respectively. Figure 2 is the schematic diagram of these two separate micelles and the monomer distribution. It is inferred that in the inverse emulsion of $SCCO_2$, most aniline hydrochloride were solubilized at micelles/water interface. Goklen (31) researched the influence of solvent on the maximum micelle dimension in inverse emulsion, they found weak polarity of solvent led to an increasing of number and a reduction of dimension of micelles. $SCCO_2$ has much lower surface tension than isooctane (9), so the dimension of reverse micelles in $SCCO_2$ was much smaller and there was much bigger $SCCO_2$/water interface area. Thus, more surfactant molecules were needed in $SCCO_2$ compared to isooctane with the same water content. In this case, compared to that in isooctane, more amphiphilic aniline hydrochloride monomer transfered from inside of micelles to $SCCO_2$/water interface to act as surfactant, and more monomer were exposed to $SCCO_2$.

3.2 FTIR Spectra of PANI-SC and PANI-CON

In the FTIR spectra of Figure 3, The peaks at 1566 cm^{-1} and 1489 cm^{-1} correspond to the stretching vibration of C=C in quinone-ring and benzene-ring, respectively. The peak at 1300 cm^{-1} and 1248 cm^{-1} are the characteristic of the conducting protonated form and interpreted as a $C-N^+\bullet$ stretching vibration in the polaron structure. The peaks at 1140 cm^{-1} are assigned to π-electron delocalization induced in the polymer by protonation and stretching vibration of the $C=NH^+$ structure, which is formed during protonation. The peak at 808 cm^{-1} is related to the deformation vibration of the C–H out of the plane (32). In the spectrum of PANI-SC as shown in Figure 3a, peak at

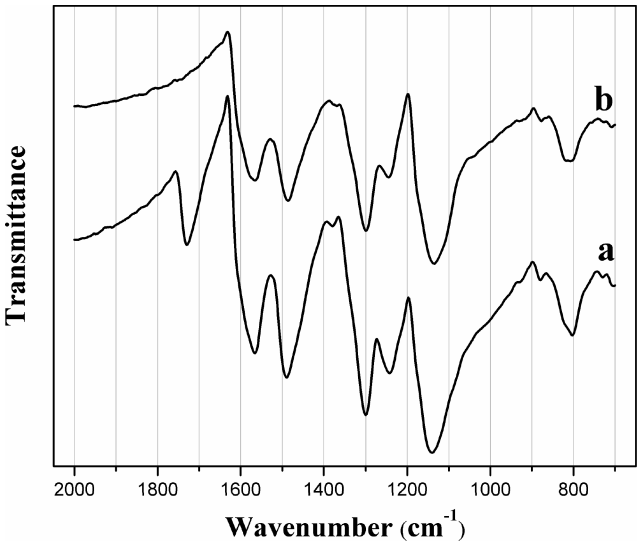

Fig. 3. FTIR spectra of PANI (a) PANI-SC; (b) PANI-CON.

about 1727 cm^{-1} corresponds to C=O in AOT can be observed. It is implied that AOT has incorporated with PANI. A slight red shift of these peaks by comparison with their position of neat surfactant (at about 1737 cm^{-1}) illustrates a more intimate interaction between PANI and AOT. But in the spectrum of PANI-CON as shown in Figure 3b, no this peak appears. In the case of conventional inverse emulsion polymerization in isooctane, the AOT could hardly incorporate into PANI, and therefore no the peak of C=O appears in the spectrum of PANI-CON. (32) In the case of inverse emulsion in $SCCO_2$, because $SCCO_2$ is an excellent plasticizer for polymer, (33) it is presumed $SCCO_2$ could plasticize the PANI molecular chain which exposed to $SCCO_2$ effectively, it caused AOT to be more likely to incorporate into PANI, thus the peak of C=O appears in the spectrum of PANI-SC.

In addition, there are no peaks belonging to another nonionic surfactant PeSi in the spectra of either PANI-SC or PANI-CON, which indicate all surfactants simply mixed with PANI have been removed. It is suggested that AOT has incorporated with PANI by interionic attraction between the positive charge in PANI molecular chain and the anion of AOT. In this case, AOT was a dopant for PANI, instead of a simple component of mixture.

3.3 SEM and TEM Analysis of PANI-SC and PANI-CON

The microstructure of PANI synthesized by inverse emulsion polymerization can be designed and controlled using surfactant assembly. Different aggregate shapes depend on the microemulsion/micellar composition, expressed through water solubilization factor w_0 ($w_0 = [H_2O]/[\text{sufactant}]$). In the conventional inverse

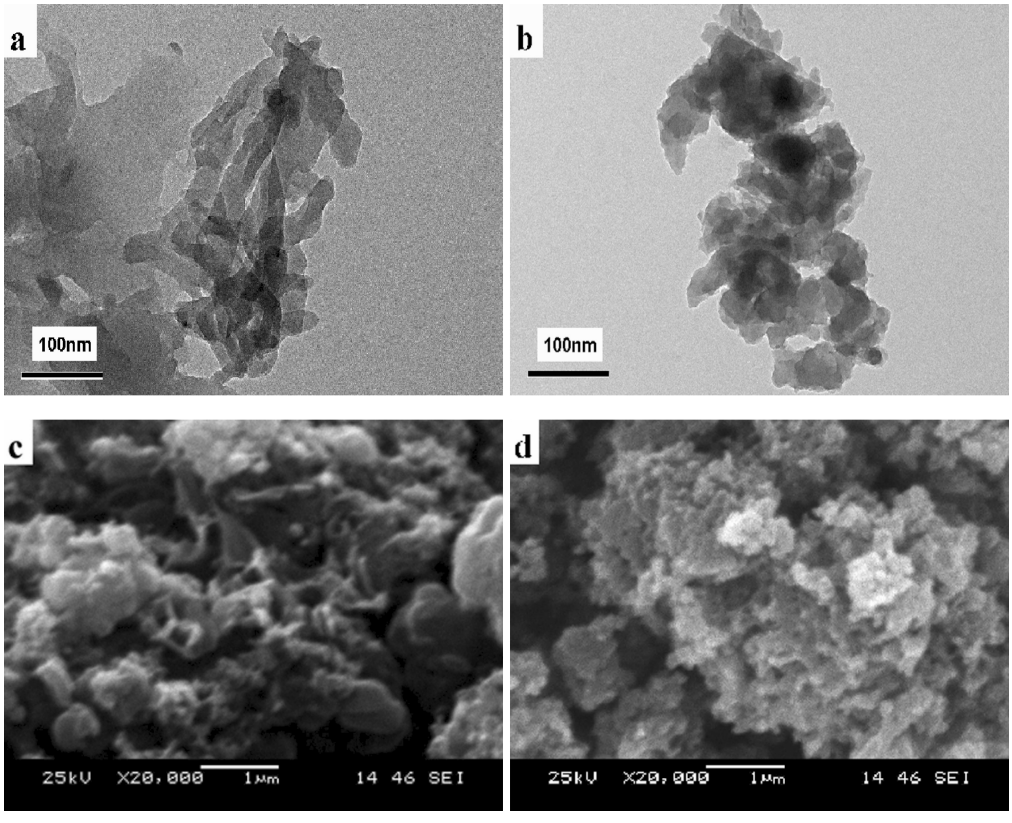

Fig. 4. TEM images of PANI (a) PANI-SC (b) PANI-CON and SEM images of PANI (c) PANI-SC (d) PANI-CON.

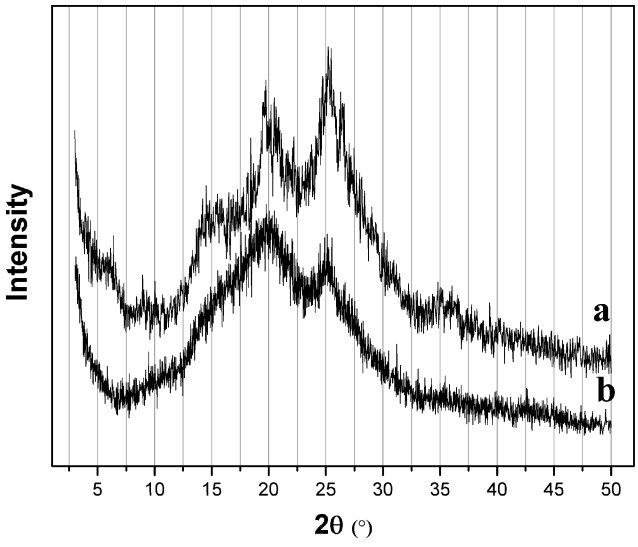

Fig. 5. XRD patterns of PANI (a) PANI-SC; (b) PANI-CON.

emulsion of isooctane, when w_0 value is smaller ($w_0 < 22.3$), needle-like PANI is expected to form, when w_0 value is higher ($w_0 > 22.3$), flakes-like PANI is yielded (34). In our experiment, for the inverse emulsion of $SCCO_2$, the w_0 value was 74. As stated in section 3.1, the dimension of micelles was much smaller than that in isooctane, and a more aniline hydrochloride monomer acted as surfactant to form needle-like micelles, which was similar to conventional inverse emulsion with smaller w_0 value ($w_0 < 22.3$). Therefore, the PANI-SC exhibited needle-like morphology, as shown in Figure 4a. In the case of emulsion of isooctane, the w_0 value was also 74 (>22.3), PANI-CON exhibited granule-like or flake-like morphology (34), as shown in Figure 4b. This result was also supported by SEM micrographs. Figure 4c exhibits the hollow structure aggregation assembled by needle-like PANI-SC, and Figure 4d exhibits the bedded structure aggregation assembled by granule-like or flake-like PANI-CON.

3.4 XRD Patterns of PANI-SC and PANI-CON

Some differences in XRD patterns between the PANI-SC and PANI-CON were also investigated, as shown in Figure 5. The two bands at $2\theta = 19.5^\circ$ and 25.1° are ascribed to the periodicity parallel and perpendicular to the polymer chains of PANI, respectively (35,36), which are observed for both PANI-SC and PANI-CON. These two peaks of PANI-SC are sharper than that of PANI-CON, which reveals higher crystallinity and more regular molecular segment arrangement of PANI-SC, probably owing to the plasticization of $SCCO_2$ for PANI, or assistance of the AOT for PANI orientation.

3.5 Properties of PANI-SC and PANI-CON

The average room temperature conductivity value of PANI-SC is 7.22S cm^{-1}, more than that of PANI-CON which is 0.85S cm^{-1}. The higher conductivity of both PANI-SC and PANI-CON obtained by inverse emulsion than that synthesized by other polymerization method (17, 20, 21) is due to a more homogenous protonation of the imine nitrogen and more ordered chain conformation of the polymer (37). The higher conductivity of the PANI-SC than PANI-CON was presumably attributed to the higher crystallinity of PANI-SC, the needle-like aggregation structure or the assistance of the AOT for PANI orientation (32, 38).

The dispersibility of samples in ethanol was also investigated. Figure 6a is the photo of PANI-SC (left) and PANI-CON (right) at the initial time when they were dispersed in ethanol, and Figure 6b is the image of them after 72 h. The ethanol dispersion of PANI-SC remained uniform and clear, but almost all PANI-CON nanoparticles had settled to the bottom (see the inset of photo) and the color of dispersed liquid was lighter than that before 72 h. PANI nanoparticles are apt to agglomerate due to the interchain π-π interaction and hydrogen bonding before they settle in agglomeration form (39). PANI-SC nanoparticles possessed a more hollow and porous configuration, and they were more likely to be buoyed in medium. Furthermore,

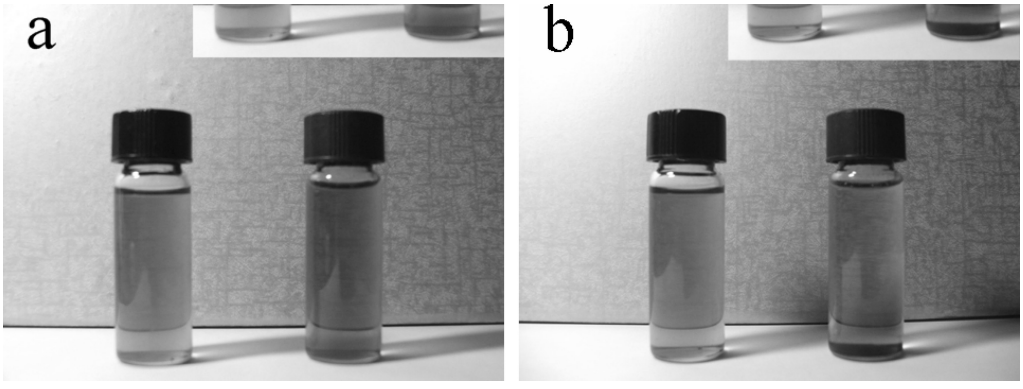

Fig. 6. photos of PANI-SC (left sample) and PANI-CON (right sample) dispersed in ethanol, (a) initial status; (b) after 72 h.

Table 1. Physical data for modified MMT clays

MMTs	*Modifying Cations*	*d Spacing(nm)*[a]	*Modifier Intercalated(wt%)*[b]
NaMMT	Na^+	1.38	N/A
Organic MMT(OMMT)	$CH_3(CH_2)_{15}N^+(CH_3)_3$	1.66	35.9
Fluorinated MMT(FMMT)	$CF_3(CF_2)_7SO_2NH(CH_2)_3N^+(CH_3)_3$	1.47	36.7

[a]Determined by XRD. [b]Determined by TGA.

AOT have incorporated into PANI molecular chain, the dissolution of hydrocarbon chain of AOT in ethanol could assist in the dispersion of PANI nanoparticles.

3.6 Preparation of PANI-FMMT-SC and PANI-OMMT-CON

PANI-FMMT and PANI-OMMT nanocomposites were prepared by intercalative polymerization in $SCCO_2$ and isooctane, respectively. Kim (40) and Shen (41) researched the polymer-MMT composites synthesized via inverse emulsion pathway method. In our experiment, FMMT was modified by a fluorinated quaternary ammonium salt in which the fluorinated tail is CO_2-phillic and thus, it can help provide steric stabilization in $SCCO_2$. In this case, FMMT platelets can be dispersed in $SCCO_2$ and is inclined to be absorbed at $SCCO_2$/water interface (10,42). On the other hand, $SCCO_2$ can impregnate, and disaggregate FMMT, and facilitate the transport monomer into FMMT interlayers. In contrast, isooctane is only an inert solvent for its bigger molecular size, lower diffusion rate, and poorer compatibility with monomer, therefore, OMMT cannot be impregnated, disaggregated and dispersed by isooctane availably, and monomer cannot be transported into OMMT interlayers effectively in the inverse emulsion of isooctane.

3.7 FTIR Spectra of Modified MMTs

The physical data for modified MMT clays can be seen in Table 1. The increasing of basal spacing of FMMT and OMMT compared to pristine NaMMT, and the modifier content intercalated into MMT suggested the introduction of fluorocarbon chain and alkyl chain into FMMT and OMMT respectively. FTIR spectra of MMTs are expressed in Figures 7 and 8. We can observe characteristic bands at 1035 cm^{-1} and 1640 cm^{-1} assigned to the Si—O and —OH in MMTs. The peaks at 2920 cm^{-1}, 2850 cm^{-1} and 1470 cm^{-1} in spectrum (b) corresponding to C—H groups, confirmed the presence of alkyl chain in OMMT. The peaks at 1365 cm^{-1} in spectrum (c) corresponding to O=S=O groups, 1209 cm^{-1}, 1150 cm^{-1} in spectrum (c) corresponding to $>CF_2$, $-CF_3$ groups confirmed the existence of fluorocarbon chain in FMMT.

3.8 XRD Patterns of PANI-FMMT-SC and PANI-OMMT-CON

Figure 9 shows the XRD diffraction patterns of PANI-FMMT-SC with different FMMT loadings. There is a lack of any diffraction peak for these composites in $2\theta = 2$–10° as the FMMT loading was 3 wt% or 12 wt% to monomer,

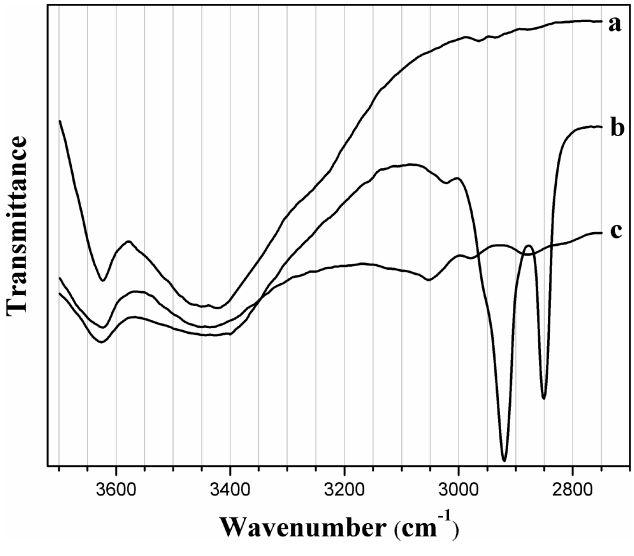

Fig. 7. FTIR spectra of MMTs (2750 cm^{-1} −3700 cm^{-1}), (a) NaMMT; (b) OMMT; (c) FMMT.

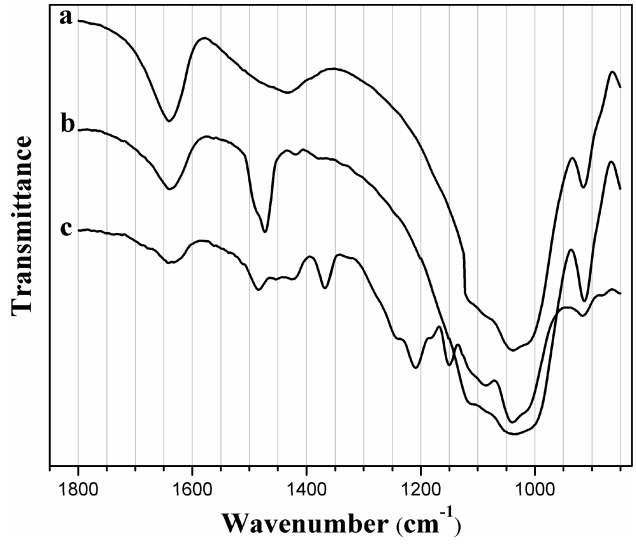

Fig. 8. FTIR spectra of MMTs (850 cm^{-1} −1800 cm^{-1}), (a) NaMMT; (b) OMMT; (c) FMMT.

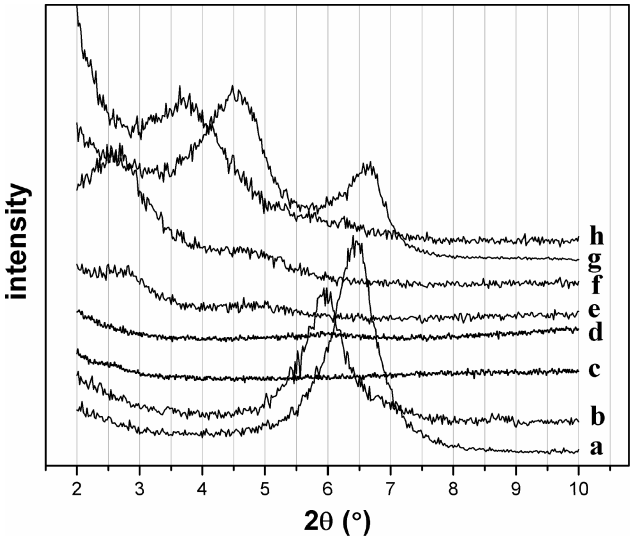

Fig. 9. XRD patterns of MMTs and PANI-MMTs, (a) NaMMT; (b) FMMT; (c) PANI-FMMT3-SC; (d) PANI-FMMT12-SC; (e) PANI-FMMT25-SC; (f) PANI-FMMT50-SC; (g) OMMT; (h) PANI-OMMT12-CON.

which indicates that the fully delaminated FMMT platelets were dispersed in composite through the intercalation and polymerization. Even if FMMT loading was increased to 25 wt% or 50 wt%, the XRD patterns show almost invisible peaks or relatively weaker peaks at lower 2θ angle ($2\theta = 2.7°$d spacing = 3.30 nm) as opposed to the peak of unintercalated FMMT at higher 2θ angle ($2\theta = 6.0°$d spacing = 1.47 nm), which suggests the composites with effectively intercalated FMMT were obtained. This result is attributed to the affinity of fluorocarbon molecular chain in FMMT and $SCCO_2$. FMMT was dispersed homogeneously in $SCCO_2$ and FMMT can also itself serve as a stabilizer for reverse micelles, monomer and polymer (10, 42), which led to more opportunity for monomer to diffuse into FMMT.

It is also noteworthy that a little shift and obvious strong peak can be observed in the XRD pattern of PANI-OMMT-CON at 12 wt% OMMT loading, it resulted from the fact that OMMT was partially intercalated in isooctane, since isooctane is an inert medium for intercalation of MMT and monomer, as stated in section 3.6.

3.9 TEM Analysis of PANI-FMMT-SC and PANI-OMMT-CON

The dispersion microstructure of the intercalated FMMT layers was also examined by means of TEM. The microstructure of PANI-FMMT12-SC, PANI-FMMT25-SC and PANI-OMMT-CON are shown in Figures 10a, 10b and 10c, respectively. The dark lines represent the cross section of the MMT layers. We find the FMMT in nanocomposites have been fully delaminated and the nanoscale FMMT platelets were dispersed in PANI-FMMT-SC homogeneously, but OMMT in PANI-OMMT-CON still remained a layered structure, which are in good agreement with the XRD result. The facilitation for preparation of nanocomposites with highly concentrated and effectively dispersed MMT in $SCCO_2$ is confirmed again.

3.10 Thermal Stability of PANI-FMMT-SC and PANI-OMMT-CON

Figures 11 and 12 show the TG and DTG curves of pure PANI, PANI-OMMT-CON and PANI-FMMT-SC. In the TG curves of Figure 11, the first weight losses below 100°C were presumably a result of the water or hydrogen chloride released for all the samples. The gradual weight losses are observed at the temperature above 200°C for all samples, revealing PANI itself was decomposed thermally within this temperature range. It is obvious in Figures 11, 12 that the total thermal weight loss and the thermal degradation rate of PANI-FMMT-SC were much lower than that of PANI-OMMT-CON, and the corresponding temperature of maximum degradation rate of PANI-FMMT-SC was lower than that of PANI-OMMT-CON. PANI-FMMT-SC nanocomposite exhibited excellent thermal stability owing to the fully delaminated and highly dispersed FMMT platelets, which induced a tortuous pathway for volatile degradation products or a barrier for the movement of PANI molecular chain, and there might be larger area interactions between polymer chain and FMMT (43, 44).

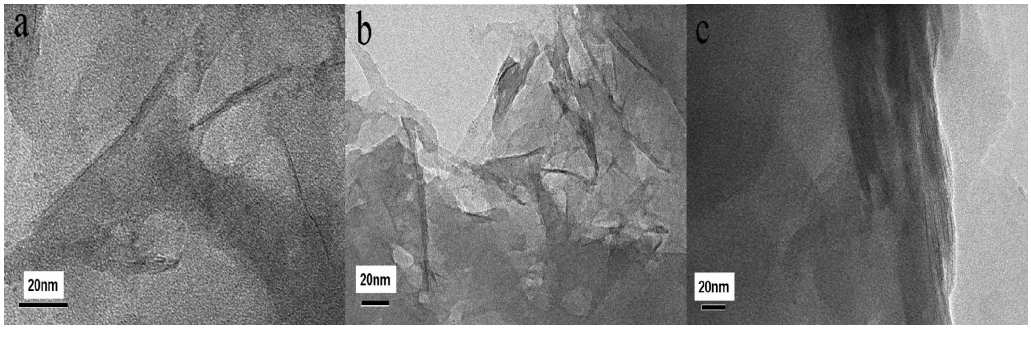

Fig. 10. TEM images of PANI-MMTs, (a) PANI-FMMT12-SC; (b) PANI-FMMT25-SC; (c) PANI-OMMT12-CON.

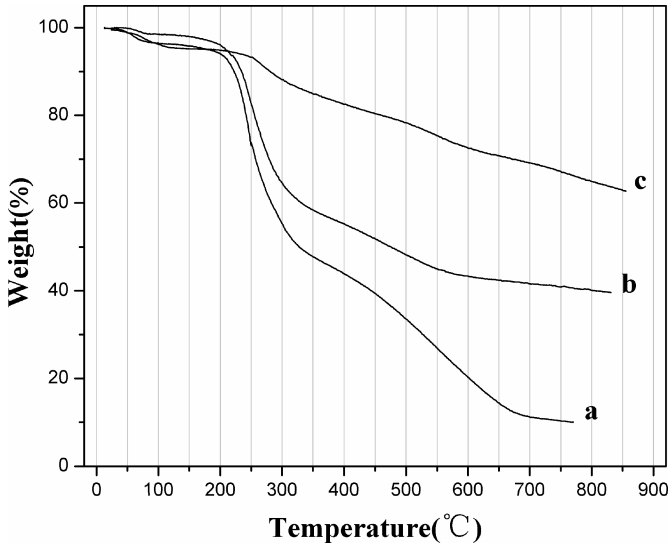

Fig. 11. TGA curves of PANI and PANI-MMTs, (a) pure PANI; (b) PANI-OMMT12-CON; (c) PANI-FMMT12-SC.

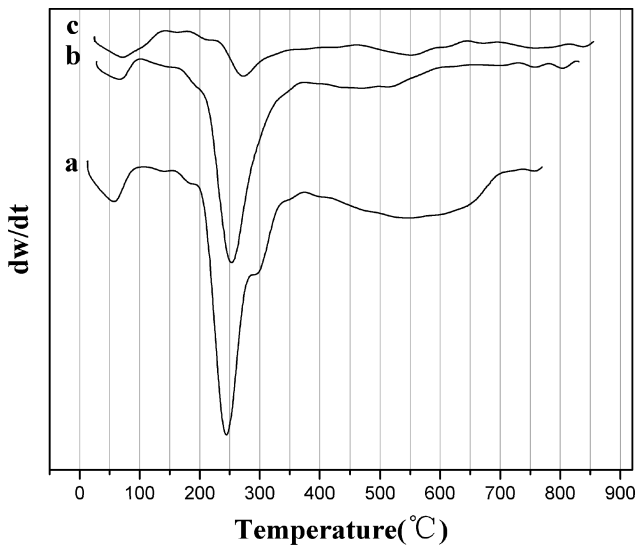

Fig. 12. DTG curves of PANI and PANI-MMTs; (a) pure PANI; (b) PANI-OMMT12-CON; (c) PANI-FMMT12-SC.

4 Conclusions

A new procedure with the aid of reverse micelles in $SCCO_2$ was successfully employed to synthesize PANI and PANI-FMMT nanocomposites. The PANI with a more favorable aggregation structure, higher crystallinity, more excellent conductivity and better dispersibility in ethanol was synthesized in $SCCO_2$. Furthermore, the PANI-FMMT nanocomposites with highly loading, fully delaminated FMMT were also prepared in $SCCO_2$. PANI-FMMT prepared in $SCCO_2$ was superior to PANI-OMMT prepared in isooctane on the intercalation of MMT, owing to the effective impregnation, disaggregation and delamination of FMMT in $SCCO_2$. PANI-FMMT exhibited the remarkable improvement on thermal stability compared with pure PANI and PANI-OMMT. It is concluded that $SCCO_2$ is not only an "alternative" solvent for its environmental-friendly characteristic but also an "effective" medium to prepare some intercalative composite materials.

Acknowledgments

We gratefully acknowledge financial support for this project by the National Natural Science Foundation of China (20674017) and Shanghai Leading Academic Discipline Project (B502).

References

1. Huang, Y.Q., Schricker, S.R., Culbertson, B.M. and Olesik, S.V. (2002) *J. Macromol. Sci., Part A: Pure and Appl. Chem.*, 1&2, 27.
2. Ortega, I.A.Q., Lima, E.V., Gupta, R.B., Barcenas, G.L. and Penlidis, A. (2007) *J. Macromol. Sci., Part A: Pure and Appl. Chem.*, 44, 205.
3. Zhang, D.H., Mishima, K., Matsuyama, K., Zhou, L. and Zhang, S.B. (2007) *J. Appl. Polym. Sci.*, 103, 2425.
4. Yoshida, E. and Nagakubo, A. (2007) *Colloid Polym. Sci.,* 285, 441.
5. Galia, A., Giaconia, A. Scialdone, O., Apostolo, M. and Filardo, G. (2006) *J. Polym. Sci., Part A: Polym. Chem.*, 44, 2406.
6. Okubo, M., Fujii, S. and Minami, H. (2004) *Prog. Colloid Polym. Sci.*, 124, 121.
7. Tan, B., Lee, J.Y. and Cooper, A.I. (2007) *Macromolecules*, 40, 1945.
8. Ye, W.J. and DeSimone, J.M. (2005) *Macromolecules*, 38, 2180.
9. Jikei, M., Yasuda, H. and Itoh, H. (2007) *Polymer*, 48, 2843.
10. Zhao, Q. and Samulski, E.T. (2005) *Macromolecules*, 38, 7967.
11. Zhao, Q. and Samulski, E.T. (2006) *Polymer*, 47, 663.
12. Zerda, A.S., Caskey, T.C. and Lesser, A.J. (2003) *Macromolecules*, 36, 1603.
13. Li, J.B., Xu, Q., Peng, Q., Pang, M.Z., He, S.Q. and Zhu, C.S. (2006) *J. Appl. Polym. Sci.*, 100, 671.
14. Yan, C., Ma, L. and Yang, J.C. (2005) *J. Appl. Polym. Sci.*, 98, 22.
15. Huang, J., Virji, S., Weiller, B.H. and Kaner, R.B. (2003) *J. Am. Chem. Soc.*, 125, 314.
16. Kulkarni, M.V., Viswanath, A.K. and Khanna, P.K. (2006) *J. Macromol. Sci., Part A: Pure and Appl. Chem.*, 43, 759.
17. Kim, S.J., Lee, N.R., Yi, B.J. and Kim, S.I. (2006) *J. Macromol. Sci., Part A: Pure and Appl. Chem.*, 43, 497.
18. Bandara, W.M.A.T., Krishantha, D.M.M., Perera, J.S.H.Q., Rajapakse, R.M.G. and Tennakoon, D.T.B. (2005) *J. Compos. Mater.*, 39, 759.
19. Li, Y.F., Wang, Y.P., Gao, X.H. and Gao, J.M. (2006) *J. Macromol. Sci., Part A: Pure and Appl. Chem.*, 43, 405.
20. Salahuddin, N., Ayad, M.M. and Ali, M. (2008) *J. Appl. Polym. Sci.*, 107, 1981.
21. Çelik, M. and Önal, M. (2007) *J. Polym. Res.,* 14, 313.
22. Çelik, M. and Önal, M. (2006) *J. Macromol. Sci., Part A: Pure and Appl. Chem.*, 43, 933.
23. Quintela, L.M.A. and Rivas, J. (1993) *J. Colloid Interface Sci.*, 158, 446.
24. Marie, E., Rothe, R., Antonietti, M. and Landfester, K. (2003) *Macromolecules*, 36, 3967.
25. Kim, B.J., Oh, S.G., Han, M.G. and Im, S.S. (2000) *Langmuir*, 16, 5841.

26. Hutton, B.H., Perera, J.M., Grieser, F. and Stevens, G.W. (2001) *Colloids Surf., A*, 189, 177.
27. Eastoe, J., Paul, A., Nave, S., Steytler, D.C., Robinson, B.H., Rumsey, E., Thorpe, M. and Heenan, R.K. (2001) *J. Am. Chem. Soc*., 123, 988.
28. Liu, J.C., Shervani, Z., Raveendran, P. and Ikushima, Y. (2005) *J. Supercrit. Fluids*, 33, 121.
29. Fink, R. and Beckman, E.J. (2000) *J. Supercrit. Fluids*, 18, 101.
30. Kemmere, M.F., Meyer, T. Supercritical Carbon Dioxide in Polymer Reaction Engineering, WILEY-VCH Verlag GmbH & Co. KGaA: Weinheim, 150, 2005.
31. Goklen, K.E. and Hatton, T.A. (1985) *Biotechnol. Progr*., 1, 69.
32. Zhou, Q., Wang, J.W., Ma, Y.L., Cong, C.B. and Wang, F. (2007) *Colloid Polym. Sci*., 285, 405.
33. Shieh, Y.T., Su, J.H., Manivannan, G., Lee, P.H.C., Sawan, S.P. and Spall, W.D. (1996) *J. Appl. Polym. Sci*., 59, 695.
34. Mani, A., Selvan, S.T., Phani, K.L.N. and Pitchumani, S. (1998) *J. Mater. Sci. Lett*., 17, 385.
35. Zhang, L. and Wan, M. (2003) *Adv. Funct. Mater*., 13, 815.
36. Yang, C.H., Chih, Y.K., Cheng, H.E. and Chen, C.H. (2005) *Polymer*, 46, 10688.
37. Zheng, W., Angelopoulos, M., Epstein, A.J. and MacDiarmid, A.G. (1997) *Macromolecules*, 30, 7634.
38. Stejskala, J., Omastova, M. and Fedorova, S. (2003) *Polymer*, 44, 1353.
39. Long, S.M., Brermeman, K.R., Saprigin, A., Kohlman, R.S., Epstein, A.J., Angelopoulos, M., Buchwalter, S.L., Rossi, A., Zheng, W. and MacDiarmid, A.G. (1997) *Synth. Met*., 84, 809.
40. Kim, J.W., Liu, F., Choi, H.J., Hong, S.H. and Joo, J. (2003) *Polymer*, 44, 289.
41. Shen, J., Cao, X. and Lee, L.J. (2006) *Polymer*, 47, 6303.
42. Voorn, D.J., Ming, W. and van Herk, A.M. (2006) *Macromolecule*s, 39, 2137.
43. Yoshimoto, S., Ohashi, F., Ohnishi, Y. and Nonami, T. (2004) *Synth. Met*., 145, 265.
44. Burnside, S.D. and Giannelis, E.P. (1995) *Chem. Mater.,* 7, 1597.